

Observation of mesoscopic quantum tunneling of the magnetization in systems with strong random magnetic anisotropy

J. I. Arnaudas, A. del Moral, and C. de la Fuente

Laboratorio de Magnetismo, Departamento de Física de la Materia Condensada and Instituto de Ciencia de Materiales de Aragón, Universidad de Zaragoza and Consejo Superior de Investigaciones Científicas, 50009 Zaragoza, Spain

P. A. J. de Groot

Physics Department, University of Southampton, Southampton SO9 5NH, United Kingdom

(Received 15 July 1992; revised manuscript received 30 November 1992)

Relaxation of the remanence of the random-magnetic-anisotropy $(\text{Gd}_{1-x}\text{Tb}_x)_2\text{Cu}$ ($x \geq 0.2$) amorphous alloys has been measured between 1.7 and 60 K. The time dependence of remanent magnetization has been found to closely follow a $\ln t$ dependence for the whole series, and the magnetic viscosity S has been obtained as a function of the temperature and concentration x . The dependence of S with the temperature is linear and shows a nonzero intercept at 0 K for the compounds with concentrations higher than $x = 0.2$. This indicates the existence of relaxation at zero temperature for these samples and points to a mesoscopic-scale quantum tunneling in three-dimensional systems with strong random magnetic anisotropy. The average tunneling volumes have been determined and they have been found to be of the order of the short-range ferromagnetically correlated volumes existing in these systems.

I. INTRODUCTION

In a series of recent papers,¹⁻⁶ it has been shown that, under certain circumstances, there is a non-null probability of observing macroscopic quantum tunneling (QT) in different magnetic systems. The effects predicted are the tunneling of the magnetization for ferromagnetic or antiferromagnetic small particles through the magnetic anisotropy energy barrier; quantum nucleation within a homogeneous region in bulk ferromagnets; and the tunneling of pinned domain walls through their pinning energy barriers. Up to now, several authors have reported experimental evidence of macroscopic QT in ferromagnetic⁷ and antiferromagnetic⁸ small particles, single-domain particles,⁹ bulk ferromagnets,¹⁰ magnetic grains,¹¹ and weak random magnets.¹²⁻¹⁴ Common features of the studied systems are a high anisotropy and/or small particle volumes, depending on the kind of magnetic materials. These conditions lead to a reasonably high rate of quantum transitions and to finite crossover temperatures from the thermal to the quantum regimes.^{1-3,5,6} It should also be noted that for most of these experimental results, the number of spins involved in the tunneling event is $\sim (4 \times 10^2) - 10^4$, indicative of mesoscopic, rather than of macroscopic scale, quantum phenomena.^{5,10}

In the present work, we report on the observation of mesoscopic QT for a different kind of magnetic system, in particular for the amorphous (*a*) $(\text{Gd}_{1-x}\text{Tb}_x)_2\text{Cu}$ random magnetic anisotropy (RMA) magnets, where some of the conditions favoring macroscopic QT of the magnetization are accomplished. This is so because of the large anisotropy due to the Tb^{3+} ions, which are, indeed, randomly distributed along the sample, as well as due to the fact that, for strong RMA systems, there exists short-

range ferromagnetic order, over distances similar to the short-range structural order correlation length R_a , within which the local anisotropy easy axes are correlated.¹⁵ Because, in amorphous systems, this length is usually of the order of several atomic distances, we considered the possibility of having a system in which the "particle" size was $\sim R_a$, certainly small, and also comparable to the size of the small ferromagnetic particles mentioned above.

Very recently we have investigated the magnetic behavior of *a*- $(\text{Gd}_{1-x}\text{Tb}_x)_2\text{Cu}$ compounds.¹⁶⁻¹⁹ From high-field magnetization, low-field ac and dc susceptibilities, and also magnetostriction measurements, we have concluded that a RMA is present even for very low Tb contents ($x \approx 0.05$). Nevertheless it is necessary to raise Tb concentrations to $x \geq 0.2$ in order to see the effects of a strong RMA (e.g., the magnetization is difficult to saturate, there are high coercive fields, etc.). Explicitly, for high Tb contents, enormous local random anisotropy D to exchange J energy ratios are reached, e.g., $D/J \approx 8.9$ for the *a*- Tb_2Cu compound.¹⁸

The study of the critical behavior allowed us to suggest the zero-field magnetic-phase diagram shown in Fig. 1, which is constituted by paramagnetic (*P*), coherent spin-glass (CSG) and spin-glass (SG) phases. It is notable that, under an applied magnetic field, the compounds with $x \leq 0.05$ behave as good ferromagnets, and those which were SG at low temperatures become, in strong enough fields, ferromagnets with wandering axes, remaining within an asperomagnetic state after the removal of the field, due to the positive exchange coupling.

Based on the thermal dependencies of the remanent magnetization and coercive field for the present systems, we had already established²⁰ that there is a change in the nature of the thermally activated processes governing the

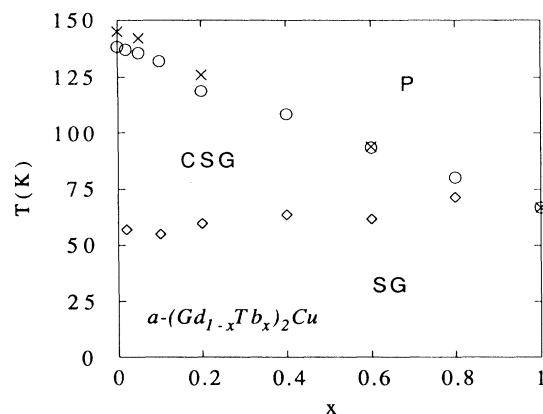


FIG. 1. Magnetic-phase diagram for the $a-(\text{Gd}_{1-x}\text{Tb}_x)_2\text{Cu}$ series. CSG is the coherent spin-glass phase, SG the spin-glass (or speromagnetic) phase, and P the paramagnetic phase. (\circ , \diamond) are from the ac low-field susceptibility measurements ($f=325$ Hz, $H_0=150$ m Oe). (\times) is from the dc low-field (1.8-Oe) susceptibility data.

low-temperature magnetic properties. Explicitly, the concentration $x \approx 0.3$ separates two regimes: exponential temperature dependence for $x > 0.3$ and a more complex algebraic behavior for $x < 0.3$. We will see below that a change in the time dependence of the remanent magnetization also occurs at around $x \approx 0.3$. Summarizing, this paper presents interesting results and conclusions concerning the relaxation of the magnetization in strong RMA systems, as well as related properties derived from their low-temperature hysterical behavior.

II. EXPERIMENTAL DETAILS

Starting from argon arc-melted polycrystalline buttons, amorphous ribbons of $(\text{Gd}_{1-x}\text{Tb}_x)_2\text{Cu}$ were prepared by melt spinning, their amorphous structure being checked by x-ray diffraction. The ribbons' thickness was around $40 \mu\text{m}$. Magnetization measurements were performed using a vibrating sample magnetometer (VSM), the magnetic field being provided by a 12-T superconducting solenoid. The magnetic field was applied in the plane of the ribbons, the measured sample being made by piling several ribbons, roughly disposed forming a star, for the sake of shape anisotropy reduction. The initial magnetic state of the samples was established by cooling in zero field from the paramagnetic regime down to the measurement temperatures. First-magnetization isotherms and their corresponding hysteresis loops were performed using a maximum applied magnetic field of 8 T, at a constant sweep rate of 200 Oe/s and at temperatures from 1.7 to 60 K. Experiments with a maximum field of 12 T were performed in order to check for any significant difference from the remanence and coercive field values as obtained for the maximum field of 8 T. However, the hysteresis loops fully close around or below this field, with no differences being observed at all. This means that the 8-T field was high enough to polarize the atomic moments and then to produce, after its suppression, an

isothermal remanent magnetization (IRM) without any memory effects. In fact, the IRM obtained using a field which closes the up and down branches of the hysteresis loop should coincide with the thermoremanent magnetization (TRM) reached under such a field.^{21,22} The measurements of the time dependence of the magnetization were performed in the remanent state, obtained after applying the maximum field of 8 T, and for a measurement time of 1800 s after the field reached zero, at measuring intervals of 2 s.

III. RESULTS AND DISCUSSION

A. Time dependence of the remanent magnetization

The time dependence of the magnetization was measured for samples with Tb concentrations of $x=1, 0.8, 0.6$, and 0.2 , at temperatures below 60 K. From the magnetic-phase diagram shown in Fig. 1, obtained from dc low-field magnetization and ac initial magnetic susceptibility measurements, it is apparent that all the present measurements were performed within the SG or speromagnetic phase. Therefore, after removing the magnetizing 8-T field, we will have an asperomagnetic remanent state, with the magnetic moments of the R^{3+} ions directed within a hemisphere. In this situation, the demagnetizing field is the only one acting upon the sample, and the magnetization will start to change with time, due to the reversal of those magnetic moments directed opposite to the demagnetizing field. Notice, however, that decay of the magnetization, either by thermal activation or QT, will take place, indeed, even in the absence of any applied magnetic field. The estimated values for the demagnetizing field range between 100 and 500 Oe, depending on the samples, for which typical dimensions are $6 \times 5 \times 0.1 \text{ mm}^3$. As can be seen in Fig. 2, the coercive field at low temperatures is quite high compared with the internal demagnetizing field at remanence, and therefore the magnetization changes, resulting from the decay of the system metastable states at these low temperatures, are necessarily very weak, typically smaller than 10^{-3}

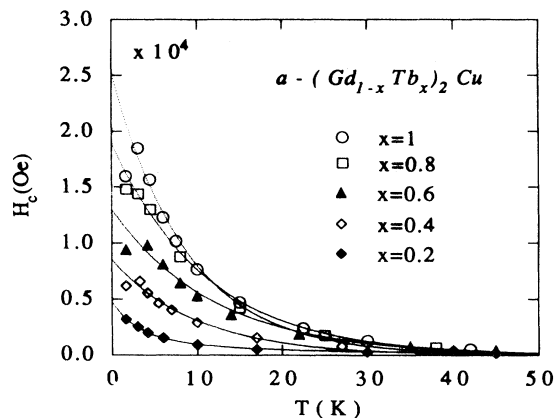


FIG. 2. Coercive field of the amorphous $(\text{Gd}_{1-x}\text{Tb}_x)_2\text{Cu}$ compounds. The lines are exponential fits for the $x=1, 0.8, 0.6$, and 0.4 alloys, and a fit to a kinks activation law for the $x=0.2$ compound (see text and Ref. 20 for details).

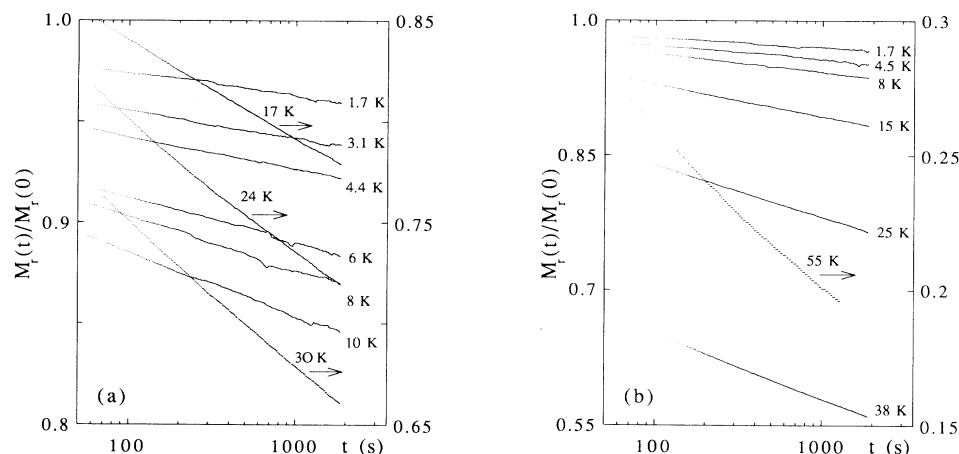


FIG. 3. Time variation of the normalized remanent magnetization of (a) amorphous Tb_2Cu and (b) amorphous $(Gd_{0.2}Tb_{0.8})_2Cu$.

emu at 1.7 K. The VSM has a sensitivity of about 10^{-5} emu, which allowed us to detect the time variation of the magnetization with great accuracy. The results obtained for all the measured samples are shown using semilog plots in Figs. 3(a) and 3(b) and 4(a) and 4(b). A vertical enlarged format was chosen in order to better show the possible departures of the experimental data from a pure logarithmic behavior. The experimental data were corrected for the time delay between the instant in which the magnetic field reaches zero and the instant in which the VSM begins to measure.

From the plots of Figs. 3(a) and 3(b) and 4(a) and 4(b), it can be immediately recognized that, for all the $a-(Gd_{1-x}Tb_x)_2Cu$ alloys studied, the time decrease of the remanence can be quite well described by a logarithmic law, i.e.,

$$M_r(t) = A - S \ln t. \quad (1)$$

Theoretically, this well-known law of magnetization variation arises from a flat-topped distribution of energy barriers (see, e.g., Refs. 23 and 24), and it has been often observed in permanent magnets,²⁵ canonical spin glasses

(for a review, see Ref. 21), and random magnetic anisotropy systems.^{22,26,27} Different distributions of barriers give other kinds of time dependencies, e.g., the algebraic decay $M(t) \sim t^{-\beta}$, resulting from an exponential distribution of energy barriers,²⁴ the Kohlrausch-Williams-Watts stretched exponential $M(t) \sim \exp(-t^{-\delta})$,²⁸ or the product of both $M(t) \sim t^{-\beta} \exp(-t^{-\delta})$.²⁹ In a recent paper,³⁰ a model of thermally activated relaxation of dispersive excitations in a percolating distribution of finite-sized domains has been developed, and the laws obtained have been used to characterize accurately the magnetization relaxation of several random systems,³⁰ as well as of ferromagnetic materials,³¹ within a wide time range (10^{-5} – 10^4 s). Various mathematical approximations to the above proposed relaxation laws, depending on the time intervals considered, reproduce the logarithmic, algebraic, and stretched exponential laws,³⁰ showing that these laws are particular cases of more general expressions. Nevertheless, for our experimental data, taken within time intervals of ~ 50 to ~ 2000 s, the logarithmic law was quite well followed. Therefore we will discard, for the sake of simplicity, the general expressions given in

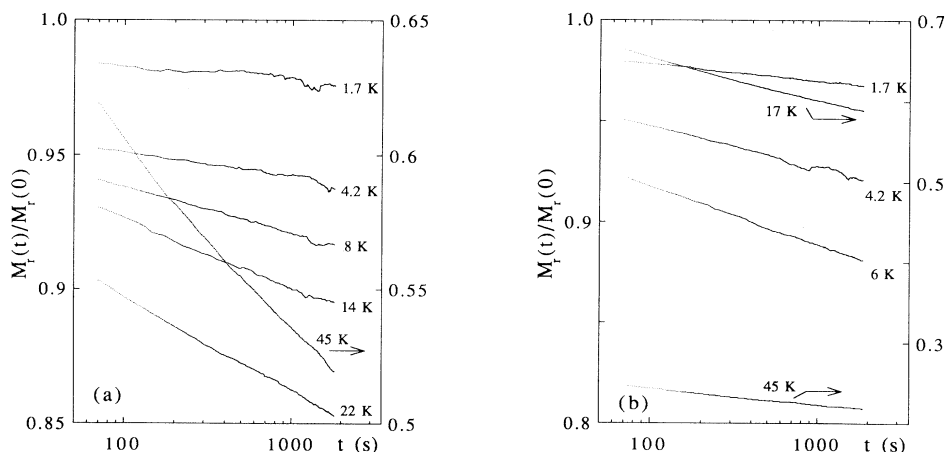


FIG. 4. Same as Fig. 3 for (a) amorphous $(Gd_{0.4}Tb_{0.6})_2Cu$ and (b) amorphous $(Gd_{0.8}Tb_{0.2})_2Cu$.

the above-mentioned work. However, we tried fittings using the stretched exponential function and the algebraic relaxation laws. Attempts to analyze our relaxation data with the stretched exponential law gave significantly less accurate fits than those obtained with the logarithmic law, but fits of similar quality, even slightly better at high temperatures, were obtained with the $t^{-\beta}$ law. This can easily be understood because of the formal equivalence of the logarithmic and algebraic laws at low temperatures. Thus, if we consider a probability distribution of energy barriers such as $P(E_a) \propto \exp(-\alpha E_a)$, and a decay for the metastable states induced by thermal activation with an Arrhenius distribution of relaxation times, i.e., $\tau = \tau_a \exp(E_a/k_B T)$, then the remanent magnetization will vary with time in the form²⁴

$$\begin{aligned} M_r(t) &\propto \int_{k_B T \ln(t/\tau_a)}^{\infty} P(E_a) dE_a \\ &= \int_{k_B T \ln(t/\tau_a)}^{\infty} \exp(-\alpha E_a) dE_a \\ &= \frac{1}{\alpha} \{ \exp[-\alpha k_B T \ln(t/\tau_a)] \} \\ &= \frac{1}{\alpha} \left[\frac{t}{\tau_a} \right]^{-\alpha k_B T} \propto t^{-\beta}, \end{aligned} \quad (2)$$

the latter expression being valid only for measuring times $t \gg \tau_a$, which is our experimental situation, where t ranges between 10 and 10^4 s, and τ_a is of the order of the spin-lattice relaxation time, i.e., $\sim 10^{-10}$ – 10^{-11} s. The algebraic law (2) reflects the fact that only the metastable states with energies

$$E_a > k_B T \ln(t/\tau_a) \approx 20 - 30 k_B T \quad (3)$$

contribute to the remanent magnetization.²⁴ The logarithmic law follows straight away from Eq. (2), provided that the β exponent ($=\alpha k_B T$) is small. Thus for low T , we have

$$M_r(t) \propto 1 - \beta \ln(t/\tau_a) \propto A - S \ln t. \quad (4)$$

A calculation of $M_r(t)$ as was done in (2), but now using for $P(E_a)$ a flat-topped distribution of width $\Delta E_a = E_a^{\max} - E_a^{\min}$, gives the same expression as Eq. (4), with $S = 2M_s k_B T / \Delta E_a$, where M_s is the saturation magnetization. Therefore, for thermally activated relaxation processes, and assuming the above distributions of barrier heights, we should expect a linear dependence with temperature for the magnetic viscosity, S , and consequently for the β exponent at low T .

In the previous discussion, we have assumed two specific probability distributions of energy barriers but, in general, the function $P(E_a)$ is unknown. It is worth mentioning that, even for a distribution $P(E_a)$ having ups and downs, the magnetization will be a smooth and decreasing function of $k_B T \ln(t/\tau_a)$, and for low T it will follow a logarithmic law for a wide time range.²⁴ However, irrespective of the form of $P(E_a)$, a magnetic viscosity S can always be defined³² through a law such as $M(t) = A - S f(t/\tau_a)$, where S is a temperature-dependent parameter which also depends upon the point of measurement on the magnetization curve and upon the

demagnetization factor of the sample.³³

To summarize, from the above discussion it is apparent that the thermal dependence of the magnetization relaxation can be adequately described through the temperature dependence of the magnetic viscosity S .

B. Thermal variation of the magnetic viscosity and 0-K viscosity

In Figs. 5(a) and 5(b) and 6(a) and 6(b), we show, for the four studied compounds, the thermal dependencies of S and β , respectively obtained from logarithmic and algebraic law fittings of the $M_r(t)$ experimental data. As expected from the theory outlined above, β and S should coincide at the lowest temperatures. The magnetic viscosity S increases linearly with T , within the temperature range of measurement, but only at the lower temperatures [Fig. 6(b)] for the $x=0.2$ compound. The thermal dependence of the β exponent has linear and quadratic variations, depending on the temperature range. This later $\beta(T)$ behavior leads to a temperature dependence for the coefficient $\alpha(T)$, in the exponential probability distribution of energy barriers used in deriving Eq. (2).

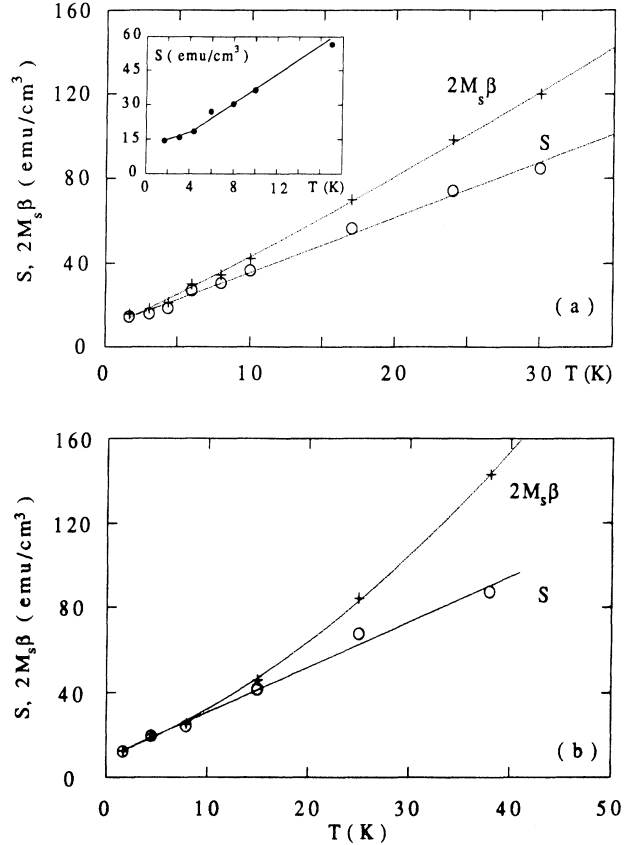


FIG. 5. Temperature dependences of the magnetic viscosity S and exponent β of the logarithmic and algebraic magnetization decay laws [expressions (1) and (2), respectively], obtained from fits of the experimental data shown in Fig. (3): (a) a -Tb₂Cu and (b) a -(Gd_{0.2}Tb_{0.8})₂Cu. The lines are linear and second-order polynomial fits for S and $2M_s\beta$, respectively. The line in the inset of (a) is a guide for the eye.

This is not unlikely, since α is related to the details of the distribution $P(E_a)$, e.g., with maximum and minimum values of the barrier heights, and these can, indeed, vary with T through the short-range ferromagnetic correlation length (see Sec. III B 1 for details). Nevertheless, keeping in mind that we are mostly interested in the low-temperature regime, where both parameters S and β coincide, in the next sections we will focus our attention only on the S parameter.

1. Quantum tunneling of the magnetization

The most striking feature of the $S(T)$ variation is the nonzero intercept at 0 K, reached from extrapolation at 1.7 K. The decay of the metastable states of the magnetization would have a null probability at zero temperature if thermal activation were the only driving process, and assuming that $P(E_a)$ is a regular function such as the flat-topped or the exponential functions described in Sec. III A. Note, however, that an energy barrier distribution $P(E_a)$ with a very high probability of vanishingly small energy barriers could lead to a considerable contribution to the magnetization decay through decay processes with large relaxation times (comparable to the measured ones). These processes would be thermally activated at low temperatures, due to the smallness of the energy barriers and, hence, the magnetization decay at low T could be due mostly to the thermal activation. Nevertheless, due to

the amorphous character of our samples, we can reasonably discard the possibility of having such a nonregular probability distribution of energy barriers in our systems. In fact, we can assume that the distribution of energy barriers is mostly due to the distribution of activation volumes, v . As we shall see below, these volumes depend on the short-range ferromagnetic correlation length that, in turn, depends on the structural correlation length R_a . So, $P(E_a)$ would be closely related to the probability distribution of structural correlation lengths. In an amorphous sample, this distribution is expected to be a regular function varying between minimum and maximum values of R_a and, therefore, we will not have a diverging function $P(E_a)$ for vanishingly small E_a . Rather, it will be like a flat distribution, as assumed in Sec. III A.

Consequently, the experimentally observed low-temperature relaxation, in agreement with the current theories, points to a quantum tunneling of the magnetization, which contributes for $x=1.0$, 0.8, and 0.6 to the decay of remanence in the present RMA systems a -(Gd_{1-x}Tb_x)₂Cu. In the case of the a -Tb₂Cu sample [see the inset in Fig. 5(a)], a tendency toward a temperature-dependent behavior of S is observed below ≈ 4 K. This result is consistent with the existence of a quantum process with a temperature-independent tunneling rate.

The crossover temperature T_Q between the thermal and quantum regimes is defined in terms of the probability for magnetization reversal, which is $P \propto \exp(-E_a/k_B T)$ for high temperatures, where thermal activation dominates, and becomes $P \propto \exp(-E_a/k_B T_Q)$ at low temperatures.¹ This crossover temperature has been calculated for QT in quite different types of magnetic systems, e.g., single-domain ferromagnetic and antiferromagnetic particles,^{1,3} for nucleation of reversed domains in ferromagnets,² in QT of domain walls,^{5,6} and (most relevant for us) in RMA systems.³⁴ For the latter,

$$T_Q = \frac{\mu_B}{k_B} \left[\frac{K}{\chi} \right]^{1/2}, \quad (5)$$

where K is the local anisotropy constant for the “particle” involved in the tunneling process, and χ the magnetic susceptibility. We can estimate K from the field necessary to close the up and down branches of the hysteresis loop H_h , using the well-known result

$$H_h = \frac{2K}{M_s}. \quad (6)$$

For a -Tb₂Cu at 1.7 K, $H_h \approx 8 \times 10^4$ Oe and $M_s \approx 1280$ emu/cm³; thus from Eq. (6) we obtain $K \approx 5.1 \times 10^7$ erg/cm³. A different estimate of K can be made using the single-ion RMA crystal-field strength for a -Tb₂Cu, i.e., $D=5.5$ K;¹⁸ the corresponding local atomic anisotropy constant, obtained from different models,^{35,36} is $D^2/J \approx 49$ K (as stated above, the ratio D/J for this system is 8.9). As we shall see below, the number of Tb³⁺ ions involved in a magnetization reversal single process at low temperatures is $N \approx 54$ in a -Tb₂Cu; now, using the random-walk argument, we can evaluate the anisotropy energy for a cluster of N atoms as $K_c = (D^2/J)\sqrt{N} \approx 360$

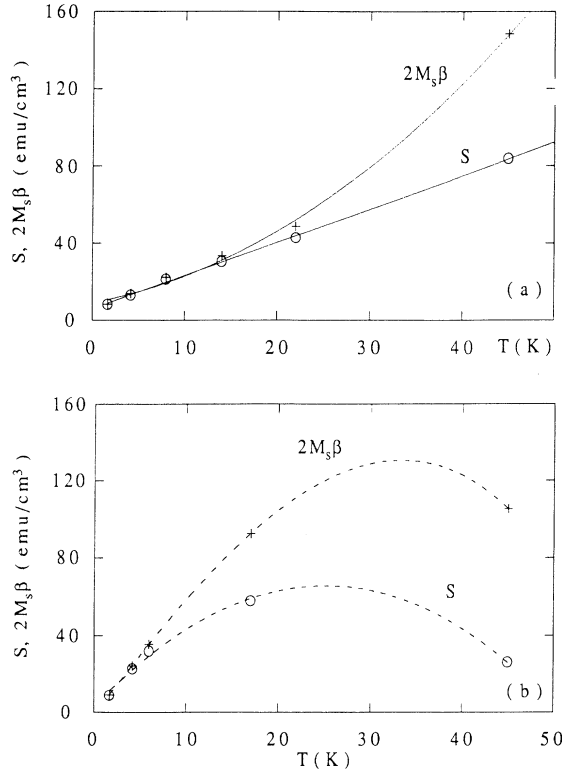


FIG. 6. (a) Same as Fig. 5(a) for a -(Gd_{0.4}Tb_{0.6})₂Cu, obtained from the experimental data shown in Fig. 4(a). (b) The same as (a) for a -(Gd_{0.8}Tb_{0.2})₂Cu from the experimental data of Fig. 4(b). In (b) the lines are guides for the eye.

K. So the corresponding volume anisotropy constant is $K \approx 5.6 \times 10^7$ erg/cm³, quite close to the value obtained using Eq. (6).

Substituting into Eq. (5) the value obtained for K and the low-temperature differential susceptibility at remanence, $\chi \approx 1.7 \times 10^{-2}$ emu/Oe cm³, we obtain $T_Q \approx 3.7$ K. The estimated crossover temperature is relatively large, certainly due to the high magnetocrystalline anisotropy introduced by the Tb³⁺ ions, and to the low magnetic differential susceptibility occurring in strong RMA systems. On the other hand, the value of T_Q derived from (5) agrees reasonably well with the experimental result [see Fig. 5(a)], which indicates a noticeable contribution from the QT process to the rate of decay of the magnetization in *a*-Tb₂Cu. In Table I, we summarize, for all the studied compounds, the values of T_Q calculated in the above-mentioned manner. Thus it is apparent that for high Gd contents, the QT regime starts at temperatures ~ 1 K, i.e., below our lowest measurement temperature 1.7 K.

2. Thermal fluctuation field and activation volumes

In order to evaluate the average volume ν of the entity, or “particle,” which tunnels, we can first give a rough estimate of its order of magnitude using expression (3) for the average activation energy at the relaxation time scale, i.e.,

$$\bar{E}_a \cong 30k_B T = K\nu, \quad (7)$$

where K is the above-considered unit volume anisotropy constant. In (7), we have neglected the influence of the magnetic field on lowering the height $K\nu$ of the energy barrier. The effect of the applied field appears in (7) as a multiplying factor of the form $\epsilon^2 \equiv g(1 - H/H_A)$, where H_A is the anisotropy field and g is a function which depends on the magnetic system and the experimental conditions [see, e.g., Ref. 37]. In our case, the field at remanence is nearly null, and always negligible compared with the coercive or anisotropy fields. We thus have $\epsilon^2 \cong g(1) = 1$. Now, from Eq. (7), using $K = 5.1 \times 10^7$ erg/cm³, we obtain $\nu \approx 320$ Å³ at $T \approx 4$ K. This volume contains about 20 Tb atoms and is only a lower limit of the actual value, as we shall see below when performing a more realistic estimate.

The magnetic viscosity defined in (1), $S = -dM/d(\ln t)$, is a magnitude which depends on the probability distribution of energy barriers in the form $S = 2M_s P(E_a) dE_a/d(\ln t) \approx 2M_s P(E_a) k_B T$ [see Eqs. (2) and (3)], and also on the experimental conditions as pointed out above.³³ Therefore, the effects of thermal activation are more precisely described in terms of the Néel fluctuation field, H_f , often referred as the coefficient of magnetic viscosity, S_ν ,^{25,32,39} and defined as

$$H_f = \frac{S}{\chi_{\text{irr}}}, \quad (8)$$

where χ_{irr} is the irreversible susceptibility. Since $\chi_{\text{irr}} = 2M_s P(E_a) (\partial E_a / \partial H)_T$,⁴⁰ the thermal fluctuation field H_f does not depend on the details of $P(E_a)$ nor on the sample and experimental peculiarities [see Eq. (9) below]. H_f is, thus, a more intrinsic parameter than S in characterizing the relaxation processes. Substituting the above expressions for S and χ_{irr} in (8), we can express H_f in terms of the field derivative of the energy barrier,²⁴

$$H_f = \frac{k_B T}{(\partial E_a / \partial H)_T}, \quad (9)$$

where the functional form of $(\partial E_a / \partial H)_T$ depends on the mechanism of magnetization reversal. Now the meaning of H_f is transparent.

From Eq. (8), we have determined the values of $H_f(T)$, using the values of $S(T)$ (Figs. 5 and 6) and the temperature dependence of χ_{irr} at remanence, obtained from the hysteresis loops [Figs. 7(a) and 7(b) and 8(a) and 8(b)] for the *a*-(Gd_{1-x}Tb_x)₂Cu compounds. The magnitudes of H_f are quite large, corresponding to the high coercive field values for these compounds according to the Barbier plot,⁴¹ in which our experimental points for H_f and H_c fit satisfactorily for $x > 0.2$, extending also the range of the plot (see Fig. 9). Note that the agreement in the Barbier plot, which is a rather general result, gives additional support to the values of the activation volumes obtained through Eq. (11). The temperature dependence of H_f for the studied samples is shown in Fig. 10, and the inset enlarged, displays the low-temperature range. The “thermal” fluctuation field H_f has non-null zero-temperature-extrapolated values for the compounds with concentrations $x > 0.2$, which account for the above-

TABLE I. Estimated crossover temperatures [from Eq. (5)] between the thermal and quantum regimes, T_Q . Characteristic temperatures for the thermal variation of the remanent magnetization, T_M , of the coercive field T_H , and of the activation volume T_ν . Temperatures below which the magnetization jumps start to appear in the hysteresis loops, T_j . Widths of the flat-topped distribution of energy barriers, ΔE_a , related to the logarithmic time dependence of the remanent magnetization. Activation volumes at 1.7 K, $\nu_{1.7}$, in Å³, and the corresponding number of Tb³⁺ ions involved. [(-): not determined].

x	T_Q (K)	T_M (K)	T_H (K)	T_ν (K)	T_j (K)	ΔE_a (K)	$\nu_{1.7}$ (Å ³)	$\nu_{1.7}$ (Tb ³⁺)
1.0	3.7	8.7	31.9	10.7	2.5	1037	895	54
0.8	3.4	11.0	38.3	11.7	5.0	1427	1347	65
0.6	3.0	12.0	49.4	14.7	7.5	1574	1741	63
0.4	—	9.8	40.6	—	6.5	—	—	—
0.2	1.1	4.2	25.0	8.0	1.7	407	1130	14

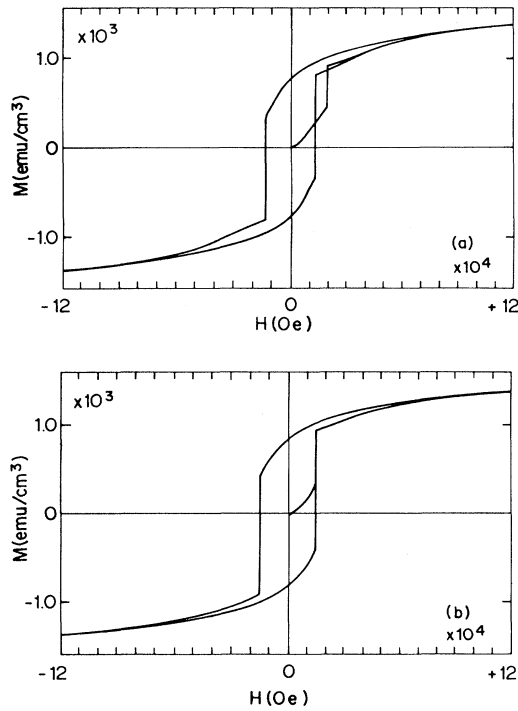


FIG. 7. Hysteresis loops at 1.7 K in (a) $a\text{-Tb}_2\text{Cu}$ and (b) $a\text{-(Gd}_{0.2}\text{Tb}_{0.8})_2\text{Cu}$, showing large jumps of the magnetization.

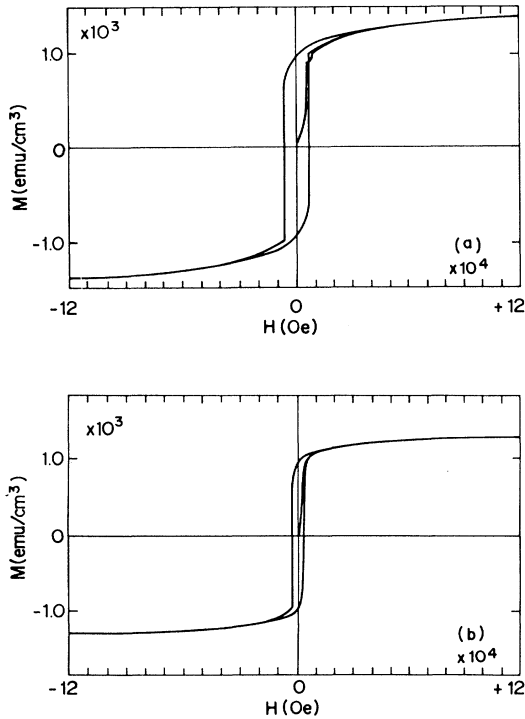


FIG. 8. Same as Fig. 7 for (a) $a\text{-(Gd}_{0.6}\text{Tb}_{0.4})_2\text{Cu}$ and (b) $a\text{-(Gd}_{0.8}\text{Tb}_{0.2})_2\text{Cu}$.

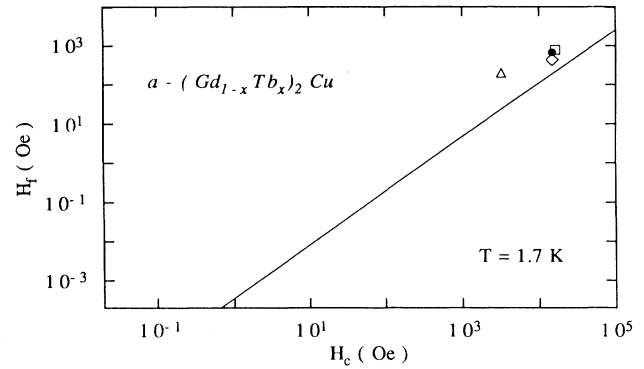


FIG. 9. Plot of the fluctuation field H_f against the coercive field H_c , at 1.7 K, for the measured compounds. (\square , $x=1$; \bullet , $x=0.8$; \diamond , $x=0.6$; \triangle , $x=0.2$). The line is the Barbier plot (Ref. 41).

mentioned observation of a quantum tunneling contribution to the low-temperature relaxation processes. We should stress that the QT contribution appears more clearly distinguished by using the $H_f(T)$ plot than the $S(T)$ plot (see Figs. 5, 6, and 10); the crossover temperature T_Q for the $a\text{-Tb}_2\text{Cu}$ compound also appears much more distinctly defined. With respect to the pure thermal contribution to H_f , i.e., $H_f(T) - H_f(0)$, all the studied alloys behave similarly with temperature. At low temperatures, there is a rapid increase of H_f , which reaches a maximum value between 3 and 8 K, depending on the samples, and then decreases more or less smoothly toward higher temperatures. The maximum showed by the fluctuation field is a common feature, already observed in other systems.^{25,38,42} This effect arises from the predominance in Eq. (9) of the factor $k_B T$ for low T , since χ_{irr} , and hence $(\partial E_a / \partial H)_T$, changes little at low temperatures, but increases rapidly at higher temperatures. The explanation below will clarify this point further.

The activation volume v can be related with $(\partial E_a / \partial H)_T$ through the above-mentioned relation $E_a = K v g (1 - H/H_A)$. The result depends on the mechanism involved in the magnetization reversal, but for the possible processes, i.e., coherent rotation, nucleation, or unpinning of domain walls, it can be shown³⁸ that

$$v \cong -C \left[\frac{\partial E_a}{\partial H} \right]_T \frac{1}{M_s}, \quad (10)$$

where C is a constant which depends on the particular reversal mechanism. In our case, we can assume that coherent rotation of the activation volume v does occur but, because we are dealing with RMA systems, the simple assumption that the applied field is antiparallel to the easy axis is certainly not applicable. Using the expression of E_a derived for a situation in which the field makes an arbitrary angle with the easy axis,³⁷ and averaging over the disorder, we have estimated that $C \approx 1.2$ for zero applied magnetic field, which is our experimental situation at remanence.

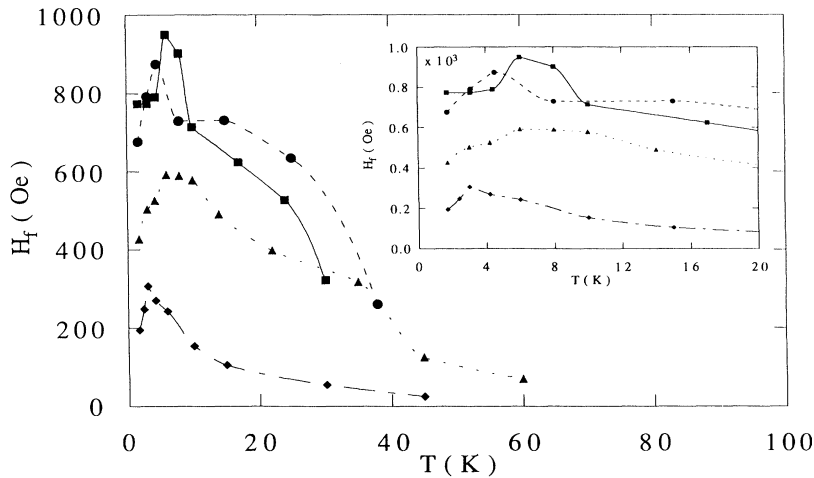


FIG. 10. The temperature dependence of the fluctuation field, H_f , of the a -($\text{Gd}_{1-x}\text{Tb}_x$) $_2\text{Cu}$ compounds. (\blacksquare , $x=1$; \bullet , $x=0.8$; \blacktriangle , $x=0.6$; \blacklozenge , $x=0.2$). In the inset, the tendency to a non-null zero-temperature intercept for $H_f(T)$ is distinguished. The lines are guides for the eye.

Substitution of (9) into (10) gives the well-known expression,^{25,32} adapted to our case, for the activation volume in terms of experimentally accessible variables:

$$\nu \cong 1.2 \frac{k_B T}{H_f M_s} \quad (11)$$

We have obtained the activation volume and its thermal dependence by substituting into (11) the values of the thermal fluctuation field calculated as $H_f(T) = [S(T) - S(0)] / \chi_{\text{irr}}(T)$. Note that from our magnetization measurements we know that, below ~ 50 K, M_s has little temperature variation and therefore it is the derivative $(\partial E_a / \partial H)_T = k_B T / H_f(T)$ which mainly accounts for the thermal dependence of ν . The subtraction of the zero intercept $S(0)$ has been performed in order to isolate the thermal contribution to the magnetization decay, since the theory outlined above deals with thermally activated processes and we have ascribed $S(0)$ to the QT process.

The temperature dependence of the activation volume for the studied samples is shown in Fig. 11. The volume

ν varies very little below ~ 10 K, and then increases quite rapidly with temperature. Its temperature variation follows an exponential dependence, i.e., $\nu \sim \exp(T/T_\nu)$, with a characteristic temperature T_ν , reported in Table I. The sizes of ν at the lowest temperature of 1.7 K vary between ~ 900 (for $x=1$) and $\sim 1700 \text{ \AA}^3$ (for $x=0.6$), which contain approximately between 54 (for $x=1$) and 65 (for $x=0.8$) Tb^{3+} ions (see Table I). Now it is interesting to compare these low-temperature activation volumes with the ferromagnetic correlation length expected for our RMA systems, if the relaxation of the magnetization is due to the reversal of correlated ion clusters.

From the determined x-ray-diffraction patterns (scattered intensity vs 2θ Bragg angle), we have estimated the mean extension of the regions producing coherent scattering. Their size L is approximately $2R_a$, i.e., twice the short-range structural order correlation length. The position and width of the first diffraction peak gives a nearest-neighbor distance of $a \approx 3.7 \text{ \AA}$ for the a - Tb_2Cu sample, in good agreement with the more refined value of

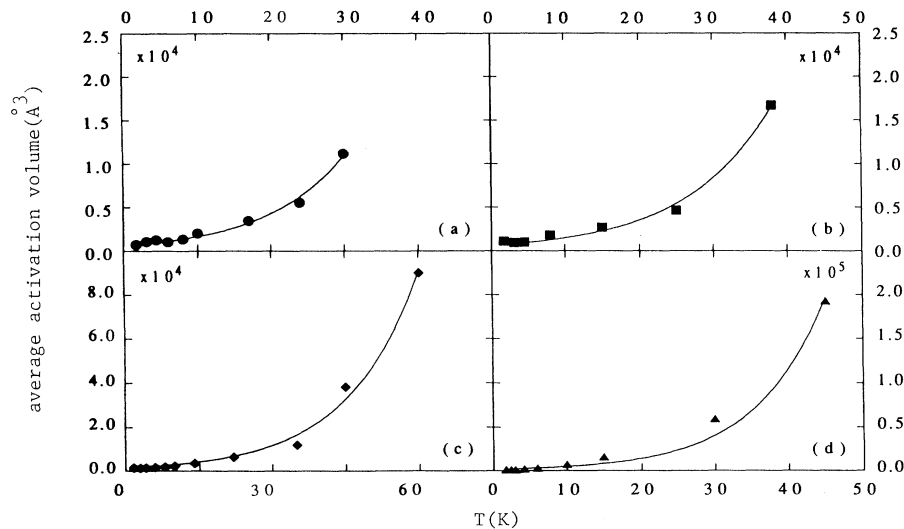


FIG. 11. Thermal variation of the average activation volume in (a) a - Tb_2Cu , (b) a -($\text{Gd}_{0.2}\text{Tb}_{0.8}$) $_2\text{Cu}$, (c) a -($\text{Gd}_{0.4}\text{Tb}_{0.6}$) $_2\text{Cu}$, (d) a -($\text{Gd}_{0.8}\text{Tb}_{0.2}$) $_2\text{Cu}$. Solid lines are exponential fits to expression $\nu = \nu(0) \exp(T/T_\nu)$.

3.5 Å obtained using neutron-diffraction techniques,⁴³ and a value of $L \approx 9.1$ Å. The value of R_a then becomes $4.5 \text{ Å} \approx 1.2a$. This means that the local easy axes are correlated only up to the first neighbors. In strong RMA systems, such as our case at low temperatures [i.e., at the SG regime (see Fig. 1)], the ferromagnetic correlation length naturally is $R_f \sim R_a$ (Ref. 15). Magnetic neutron-diffraction experiments⁴³ performed in $a\text{-Tb}_x\text{Cu}_{1-x}$ alloys, at temperatures from 1.4 to 8 K, finely confirm this point. Thus for $x \geq 0.3$, it has been found that nearly ferromagnetic order exists only up to the first neighbors (3-Å scale), although there remains some magnetic correlation up to the first three shells of neighbors (10-Å scale). These results give strong support to the size, $\sim 1500 \text{ Å}^3$, of the activation volume found at low temperatures: ν encompasses the Tb^{3+} ions which are within the ferromagnetic correlation length R_f , i.e., within the first three shells of neighbors. As anticipated, this small “particle” volume favors the probability for QT. This fact, combined with the increase of the crossover temperature T_Q , due to the strong anisotropy associated with the Tb^{3+} ions, makes the observation of quantum effects in our systems easier.

It is reasonable to assume that the low-temperature activation volumes, as deduced from the expressions for thermally activated processes, are the same volumes involved in the QT processes. Relaxation of the magnetization in other strong RMA systems has been studied in the past, e.g., in $a\text{-TbAg}$,²⁶ $a\text{-TbFe}_2$,⁴⁴ $a\text{-DyCu}$,²² and $a\text{-R}_{40}\text{Y}_{23}\text{Cu}_{37}$.²⁷ In the first two systems, thermally activated volumes of 1000 and 520 Å³, respectively, have been estimated, but no evidence of QT has been reported at all. From the temperature independence of a fast relaxation observed in $a\text{-DyCu}$ (and also in the $a\text{-R}_{40}\text{Y}_{23}\text{Cu}_{37}$ systems²⁷), Coey, McGuire, and Tissier²² suggested that QT might occur, but no estimate of the tunneling volume nor quantitative information was obtained. A stronger evidence for QT in two-dimensional (2D) RMA systems has been given by Zhang *et al.*,¹² particularly for SmCo multilayers, but, to our knowledge, this is the first time in which the activation volume in QT magnetization processes has been directly associated with the magnetic correlation length in *strong* RMA systems.

C. Concentration dependence of the relaxation characteristic temperatures, and other parameters

In an attempt to summarize the different relaxation magnitudes obtained, and to relate them to the Tb concentration, we have plotted in Fig. 12, normalized to their maximum values, the following temperatures and relevant parameters.

(i) T_M is the characteristic temperature for the thermal variation of the remanent magnetization at $t \approx 0$. The values have been obtained²⁰ from the fits of $M_r(t)$ to exponential functions for $x = 0.4, 0.6, 0.8$, and 1, and to an expression obtained for the thermal activation of narrow domain walls by formation of cylindrical “kinks” in strongly anisotropic materials,^{45,46} for $x = 0.2$.

(ii) T_H is the characteristic temperature for the thermal variation of the coercive field at $t \approx 0$, using the same pro-

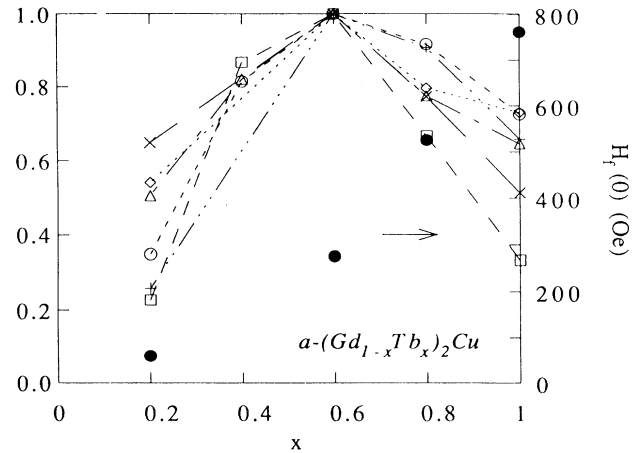


FIG. 12. Concentration dependence of normalized relaxation characteristic temperatures and other relevant parameters (see Sec. III C for definitions and Table I for absolute values). (○, T_M ; △, T_H ; ◇, T_v ; □, T_j ; +, ΔE_a ; ×, $\nu_{1.7}$). Dashed lines are guides for the eye. The extrapolated 0 K values of the fluctuation field H_f (see Fig. 10) are also shown in the figure using (●) symbols and the right-axis values.

cedures as for the T_M obtainment (see Fig. 2).

(iii) T_v is the characteristic temperature for the thermal variation of the activation volume, using pure phenomenological temperature exponential fits (see Fig. 11).

(iv) T_j is the temperature below which magnetization switching is observed in the hysteresis loops, by means of abrupt jumps between $+M_c$ and $-M_c$ (see Figs. 7 and 8).

(v) ΔE_a is the width of the flat-topped distribution $P(E_a)$ of energy barriers obtained from the slope of the $S(T)$ lines (see Figs. 5 and 6). This estimate of ΔE_a , obtained on the basis of a very simple assumption, gives the correct order of magnitude for the activation energies obtained for volumes containing ~ 100 Tb atoms.

(vi) $\nu_{1.7}$ is the activation volume at the lowest measurement temperature 1.7 K.

The actual values are given in Table I. In Fig. 12, it is clear that all the above magnitudes have similar concentration dependencies, all of them having their maximum values at $x = 0.6$. This similar dependence among the different relaxation representative parameters is not at all surprising, because they are magnitudes directly related to the thermal activation process, as is obvious for ΔE_a , or else represent processes connected with thermal activation. $k_B T_M$ and $k_B T_H$ represent activation energies for thermally activated processes, which certainly influence the temperature dependence of both the remanent magnetization and the coercive field [it should be noted, however, that $M_r(T)$ and $H_c(T)$ also depend on the thermal variation of anisotropy and exchange energies]. The average activation volume $\nu_{1.7}$ is also related to the average activation energy [see Eq. (7)]. Thus, from Fig. 12, we can say that the variation of the energy barrier with x is partially due to the variation of ν with the Tb concentration. As we pointed out above, the activation volume is of the order of R_f^3 , so that if $R_f \sim R_a$, we

can ascribe the volume variation to a variation of the structural correlation length with x . This is very likely to happen, because a reduction in $\nu_{1.7}$ by half needs only a reduction in R_a by a factor of 0.8. Thus a change in R_a from $1.2a$ (the value estimated for $x=1$) to $1.5a$ accounts for the activation volume observed in the $x=0.6$ compound. As for the T_v and T_j concentration dependencies, we have not arrived at a plausible explanation, but imagine that $k_B T_v$ and $k_B T_j$ are also connected with the activation energies of volumes varying with x as $\nu_{1.7}$ does.

From substitution of $\nu_{1.7}$ into Eq. (7), and considering that $E_a \approx \Delta E_a/2$ for the flat-topped distribution of energy barriers, we have estimated the concentration dependence of the anisotropy constant K at the lowest temperature of 1.7 K. The obtained values, which are plotted in Fig. 13, show an approximately linear decrease with x , indicating a single-ion anisotropy for these systems, as has been also shown by magnetostriction measurements.¹⁸ Moreover, the values of K at 1.7 K, obtained by means of Eq. (6), are also shown in Fig. 13. It can be seen that, although both estimates exhibit a similar x variation and give the same order of magnitude, the absolute values of K obtained from Eq. (7) are between 48% and 96% higher than those obtained from Eq. (6). This discrepancy probably arises from the simple assumptions of a squared distribution for $P(E_a)$ and a mean activation energy $\bar{E}_a \approx \Delta E_a/2$.

Using the already employed random-walk argument for the a -Tb₂Cu compound (see Sec. III B 1), we have obtained values of K at 1.7 K for the remainder of the samples. Values of $D=5.5$ K and $J=0.61$ K (Ref. 18) for the pure a -Tb₂Cu compound, *separately* obtained using a magnetoelastic model for magnetostriction in strong RMA systems,⁴⁷ have either been kept constant at $D=5.5$ K along the series or varied as a function of the concentration, $J(x)$. The x dependence of J has been obtained using the known value of $J(1)=0.61$ K and the

concentration dependence of the determined paramagnetic Curie temperatures, in the form $J(x)=J(0)(1-0.5x)$. In Fig. 13, we show the values of K obtained via this random-walk argument. In this case, the absolute values are closer to those obtained using Eq. (6), but the detailed concentration dependence does not agree. This can be due to a nonconstant crystal-field strength D along the series. The variation $D(x)$ needed in order to account for this difference is also given in Fig. 13. As can be seen, the values of D vary between ~ 5.3 and ~ 7.2 K, which nevertheless constitutes a small variation with the Tb content, indicative of a single-ion origin for the RMA. Note that some uncertainty in the closing field H_h in Eq. (6) could reduce even further the estimated variation of D with the Tb content.

In Fig. 12, we also show the extrapolated zero-temperature intercepts of the fluctuation field, $H_f(0)$. The value of $H_f(0)$ should be directly connected with the probability of QT, i.e., $P \propto \exp(-E_a/k_B T_Q)$, which, using Eqs. (5) and (7), transforms to $P \propto \exp(-\nu \chi K / \mu_B)$. If we introduce the K values deduced from (6) into this expression, along with the values of χ at remanence, and assume $\nu=\nu_{1.7}$, the result is that, at 1.7 K, P in fact increases with x , as the experimental results show. However, for $x < 1$, the calculated QT probability relative to the maximum reached at $x=1$ is negligible, against the substantial values observed for $H_f(0)$ when $x < 1$. Since the QT probability depends exponentially on the constitutive parameters ν , χ , and K , it is likely that small variations of these parameters along the series could explain the strong concentration dependence of P , and hence the values of $H_f(0)$. Clearly this point needs further work and clarification, e.g., measurements in the range of the mK , to reach more accurate values of $H_f(0)$.

IV. CONCLUSIONS

From the time dependence of remanent magnetization measurements, we have studied the magnetic viscosity of the series of strong RMA systems a -(Gd_{1-x}Tb_x)₂Cu. We have found that a non-null magnetization decay occurs when extrapolated at 0 K for the magnetic viscosity S or the fluctuation field H_f , pointing to a significant mesoscopic quantum tunneling of the magnetization at low temperatures for Tb concentrations higher than $x=0.2$. For the pure compound a -Tb₂Cu, the experimental results suggest a crossover temperature T_Q from the quantum to thermal regimes of ~ 4 K, in reasonably good agreement with the value of 3.7 K calculated from theory. Using the thermal fluctuation field, we have obtained the average activation volumes ν involved in a single tunneling event, finding $\nu \sim 900$ – 1700 \AA^3 along the series. These volumes encompass ~ 54 – 65 Tb^{3+} ions. This result is consistent with the number of ferromagnetically correlated magnetic moments, independently determined by x-ray- and neutron-diffraction⁴³ techniques. Moreover, the concentration dependence of the different characteristic temperatures and relevant parameters involved in the magnetization relaxation processes (see Sec. III C and Table I) has been explained in terms of the structural correlation length. We have also given

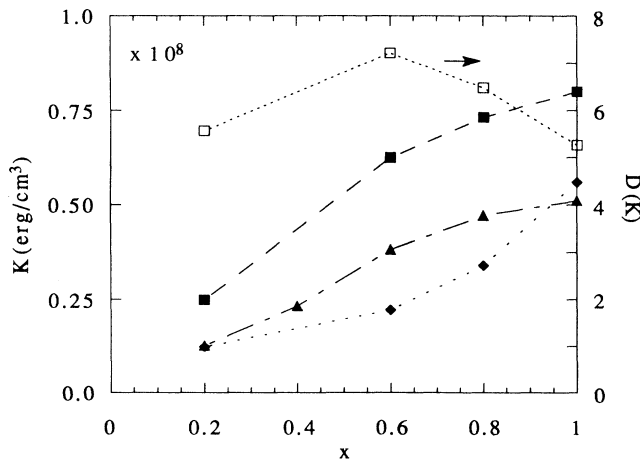


FIG. 13. The dependence on the Tb concentration of the anisotropy constant obtained from: ■, [Eq. (7)] and using $\bar{E}_a = \Delta E_a/2$; ▲, Eq. (6); ◆, the random-walk argument. The deduced variation of the crystal-field strength, D , along the series is also shown (□ symbols and right-axis values).

different estimates for the concentration dependence of the anisotropy constant, K , obtaining an approximately linear decrease of K with x , which signals a single-ion character for the anisotropy in the present series. From the random-walk argument, we have also obtained that the variation of the crystal-field strength D along the series is small, corresponding to a local single-ion anisotropy associated to the randomly distributed Tb^{3+} ions.

Although measurements in the mK range would be desirable, we believe that the results presented in this work constitute the first observation of mesoscopic quantum tunneling of the magnetization in systems having

strong single-ion random magnetic anisotropy and short-range ferromagnetic order.

ACKNOWLEDGMENTS

We are indebted to Professor J. Tejada and Professor B. Barbara for helpful discussions, to Professor E. M. Chudnovsky for a critical reading of the manuscript and a useful discussion, and to M. Ciria for help with some measurements. This work was supported by the "Acciones Integradas" Nos. 138 and 200, from the Spanish/British Joint research program, and by the Spanish DGICYT under Grant No. PB 90/1014.

- ¹E. M. Chudnovsky and L. Gunther, *Phys. Rev. Lett.* **60**, 661 (1988).
- ²E. M. Chudnovsky and L. Gunther, *Phys. Rev. B* **37**, 9455 (1988).
- ³B. Barbara and E. M. Chudnovsky, *Phys. Lett. A* **145**, 205 (1990).
- ⁴I. V. Krive and O. B. Zaslavskii, *J. Phys. Condens. Matter* **2**, 9457 (1990).
- ⁵P. C. E. Stamp, *Phys. Rev. Lett.* **66**, 2802 (1991).
- ⁶E. M. Chudnovsky, O. Iglesias, and P. C. E. Stamp, *Phys. Rev. B* **46**, 5392 (1992).
- ⁷C. Paulsen, L. C. Sampaio, B. Barbara, D. Fruchard, A. Marchand, J. L. Tholence, and M. Uehara, *Phys. Lett. A* **161**, 319 (1991); C. Paulsen, L. C. Sampaio, B. Barbara, R. Tucoulou-Tachoueres, D. Fruchart, A. Marchand, J. L. Tholence, and M. Uehara, *Europhys. Lett.* **19**, 643 (1992).
- ⁸D. D. Awschalom, J. F. Smyth, G. Grinstein, D. P. DiVicenzo, and D. Loss, *Phys. Rev. Lett.* **68**, 3092 (1992).
- ⁹L. L. Balcells, J. L. Tholence, S. Linderroth, B. Barbara, and J. Tejada, *Z. Phys. B* **89**, 209 (1992).
- ¹⁰M. Uehara and B. Barbara, *J. Phys. (Paris)* **47**, 235 (1986); B. Barbara, P. C. E. Stamp, and M. Uehara, *ibid.* **49**, C8-529 (1988).
- ¹¹L. L. Balcells, X. X. Zhang, F. Badia, J. M. Ruiz, C. Ferraté, and J. Tejada, *J. Magn. Magn. Mater.* **109**, L159 (1992); J. Tejada, X. X. Zhang, and L. L. Balcells, *ibid.* **118**, 65 (1993).
- ¹²X. X. Zhang, L. L. Balcells, J. M. Ruiz, O. Iglesias, J. Tejada, and B. Barbara, *Phys. Lett. A* **163**, 130 (1992).
- ¹³X. X. Zhang, L. L. Balcells, J. M. Ruiz, J. L. Tholence, B. Barbara, and J. Tejada, *J. Phys. Condens. Matter* **4**, L163 (1992).
- ¹⁴J. Tejada, X. X. Zhang, and E. M. Chudnovsky, *Phys. Rev. B* (to be published).
- ¹⁵E. M. Chudnovsky and R. A. Serota, *Phys. Rev. B* **26**, 2697 (1982).
- ¹⁶P. A. J. de Groot, B. D. Rainford, S. H. Kilcoyne, M. El Khadi, J. I. Arnaud, and A. Soliman, *J. Phys. (Paris)* **49**, C8-1243 (1988).
- ¹⁷J. I. Arnaud, A. del Moral, P. A. J. de Groot, B. D. Rainford, and M. El Khadi, *J. Appl. Phys.* **69**, 5786 (1991).
- ¹⁸J. I. Arnaud, A. del Moral, P. A. J. de Groot, and B. D. Rainford, *J. Magn. Magn. Mater.* **101**, 65 (1991).
- ¹⁹J. I. Arnaud, A. del Moral, P. A. J. de Groot, and C. de la Fuente, *J. Magn. Magn. Mater.* **104-107**, 216 (1992).
- ²⁰J. I. Arnaud, A. del Moral, and P. A. J. de Groot, *J. Magn. Magn. Mater.* **104-107**, 115 (1992).
- ²¹K. Binder and A. P. Young, *Rev. Mod. Phys.* **58**, 801 (1986).
- ²²J. M. D. Coey, T. R. McGuire, and B. Tissier, *Phys. Rev. B* **24**, 1261 (1981).
- ²³S. Chikazumi, *Physics of Magnetism* (Wiley, New York, 1964).
- ²⁴S.-k. Ma, *Phys. Rev. B* **22**, 4484 (1980).
- ²⁵D. Givord, A. Liénard, P. Tenaud, and T. Viadieu, *J. Magn. Magn. Mater.* **67**, L281 (1987).
- ²⁶B. Boucher and B. Barbara, *J. Phys. F* **9**, 151 (1979).
- ²⁷A. del Moral, J. I. Arnaud, B. D. Rainford, and C. Cornelius, *J. Phys. Condens. Matter* **4**, 6303 (1992).
- ²⁸R. V. Chamberlin, G. Mozurkewich, and R. Orbach, *Phys. Rev. Lett.* **52**, 867 (1984).
- ²⁹A. T. Ogielski, *Phys. Rev. B* **32**, 7384 (1985).
- ³⁰R. V. Chamberlin and D. N. Haines, *Phys. Rev. Lett.* **65**, 2197 (1990).
- ³¹R. V. Chamberlin and F. Holtzberg, *Phys. Rev. Lett.* **67**, 1606 (1991).
- ³²E. P. Wohlfarth, *J. Phys. F* **14**, L155 (1984).
- ³³R. Street, P. G. McCormick, and L. Folks, *J. Magn. Magn. Mater.* **104-107**, 368 (1992).
- ³⁴E. M. Chudnovsky (private communications).
- ³⁵R. A. Serota, *Phys. Rev. B* **37**, 9901 (1988).
- ³⁶A. del Moral and J. R. Cullen, *J. Magn. Magn. Mater.* **83**, 165 (1990); (unpublished).
- ³⁷R. H. Victoria, *Phys. Rev. Lett.* **63**, 457 (1989).
- ³⁸D. Givord, Q. Lu, and M. F. Rossignol, in *Proceedings of the NATO Advanced Study Institute on the Science and Technology of Nanostructured Magnetic Materials*, edited by G. C. Hadjipanayis and G. A. Prinz (Plenum, New York, 1991), p. 635.
- ³⁹L. Néel, *J. Phys. Radium* **12**, 339 (1951).
- ⁴⁰P. Gaunt, *Philos. Mag.* **34**, 775 (1976).
- ⁴¹J. C. Barbier, *Ann. Phys. (Paris)* **9**, 84 (1954).
- ⁴²Liu Jinfang, Luo Helie, and Wan Jiang, *J. Phys. D* **25**, 838 (1992).
- ⁴³B. Boucher, M. Sanquer, R. Tourbot, and R. Bellissent, *J. Phys. Condens. Matter* **3**, 1985 (1991).
- ⁴⁴J. J. Rhyne, J. A. Schelleng, and N. C. Koon, *Phys. Rev. B* **10**, 4672 (1974).
- ⁴⁵R. Kütterer, H. R. Hilzinger, and H. Kronmüller, *J. Magn. Magn. Mater.* **4**, 1 (1977).
- ⁴⁶T. Egami, *Phys. Status Solidi A* **19**, 747 (1973); **20**, 157 (1973).
- ⁴⁷A. del Moral and J. I. Arnaud, *Phys. Rev. B* **39**, 9453 (1989).